



# Mechanical support concept of the DEMO breeding blanket

C. Bachmann<sup>a,b,\*</sup>, C. Gliss<sup>a</sup>, T. Härtl<sup>a</sup>, F. Hernandez<sup>c</sup>, I. Maione<sup>c</sup>, T. Steinbacher<sup>a</sup>, Z. Vizvary<sup>d</sup>

<sup>a</sup> EUROfusion Consortium, PPPT Department, Garching, Boltzmannstr. 2, Germany

<sup>b</sup> Technical University of Denmark, Lyngby, Denmark

<sup>c</sup> Association KIT-Euratom, Karlsruhe Institute of Technology (KIT), Karlsruhe, Germany

<sup>d</sup> UKAEA, Culham Science Centre, Abingdon, Oxon OX14 3DB, United Kingdom

## ARTICLE INFO

### Keywords:

DEMO  
Tokamak  
Vacuum vessel  
Cryostat  
In-vessel components  
Breeding blanket

## 1. Introduction

### 1.1. Overview

A tokamak architecture based on large vertical blanket segments was – to the authors' best knowledge – first proposed in the early 80s for INTOR [2], adopted in NET [3], in the first concept of ITER [4], and in the European power plant conceptual studies [5]. This architecture aims at reducing the number of in-vessel components (IVCs) and hence their replacement duration and allows using a crane-like device to lift the heavy breeding blanket (BB) segments. Difficulties had been encountered Fig. 5 in the 1980s in the search for an attachment concept for the blanket segments made of austenitic steel of NET and ITER [4].

The basic principle of the BB attachment concept that is presented here was first introduced in [6] and has been partially verified previously based on a number of assumptions in [7].

### 1. BB-VV attachment system conceptual study

#### 1.2. Requirements

##### Loads: See chapter 3

**First wall (FW) alignment:** During operation and plasma ramp-up/ramp-down the BB FW must be accurately aligned in toroidal and poloidal direction to avoid heat load concentrations due to charged particles, e.g. on leading edges, see also [8]. Since protection limiters are

foreseen in DEMO that protrude the BB FW and therefore collect most charged particles we expect the FW alignment requirement to be reduced as compared to ITER, which has prescribed an alignment tolerance of  $\pm 5$ -10mm [9]. We assume that an alignment of the DEMO BB FW with a tolerance of  $\pm 5$ -10mm will be sufficient [10, 11].

**Electrical connections:** The requirements concerning the electrical integration of BB segments are provided in [6]:

- All IVCs must be electrically grounded to the VV
- Electrical connections between BB and VV are required in vicinity of all BB feeding pipes to avoid currents to flow through the pipes generating intolerable EM loads.
- Locations where electrical contact cannot be guaranteed shall be electrically insulated to ensure the predictability of the paths of occurring currents.
- (Electrical) contact between adjacent IVCs must be prevented if it would restrain their thermal deformation either by defining an appropriate gap size or by electrically insulating potential contact areas.

Electrical insulation at physical contact interfaces can be ensured by a surface coating. For the insulated supports of the ITER shield block Al-bronze pads with a 250 $\mu$ m thick plasma-sprayed alumina coating on all sides were qualified [12].

**BB positioning:** The support structures presented in this article require from the BB transporter a BB positioning precision of  $\sim \pm 40$ mm

\* Corresponding author.

E-mail address: [christian.bachmann@euro-fusion.org](mailto:christian.bachmann@euro-fusion.org) (C. Bachmann).

prior to the final engagement. The final engagement movements of the BB segments are guided by the BB support structures into their installed position achieving a much smaller installation tolerance, paragraph 1.5.

### 1.3. Mechanical support principles

Each blanket segment is individually supported by the VV without any physical contact to the other blankets or in-vessel components. All BB support structures are shear keys or contact pads relying on simple compressive contact for load transfer; bolts or other types of attaching locks as considered in the shield blankets of NET [13] are not used to simplify the remote maintenance operations required for the BB replacement and to avoid the integration of moveable elements in the blanket. To support the inboard segments against the very large radial loads radial supports are incorporated at three poloidal locations. The outboard segments are radially supported only at the top and at the bottom. During tokamak operation the BB segments are radially pre-compressed by the ferromagnetic force acting on the BB steel and vertically pre-compressed by obstructed thermal expansion.

#### a) Radial pre-compression by the ferromagnetic force

The radial gradient of the toroidal field (TF) generates a large radial force on the ferromagnetic blanket material EUROFER. Since the TF is constant during and in-between plasma pulses the BB support concept can rely on this force to guarantee physical contact at the radial supports with significant pre-compression. As a consequence bolts providing pre-compression as e.g. in the supports of the ITER blanket [12] are not required.

The support concept of the BB segments is that of an arch bridge where both end points of the arch are constrained. In case of a temperature increase the bow of the arch is sufficiently flexible to rise and reaction forces on the supports remain tolerable. The radial ferromagnetic force acting on the blankets corresponds to the vertical gravity force acting on the bridge, see Fig. 1, and also defines their radial position. The curved part of the otherwise straight inboard segment provides sufficient bending flexibility if the upper vertical support is located at the end point of the segment. Otherwise it would be too stiff if constructed as a single box structure with a poloidally continuous FW plate and its thermal expansion causes a steep rise of the vertical reaction

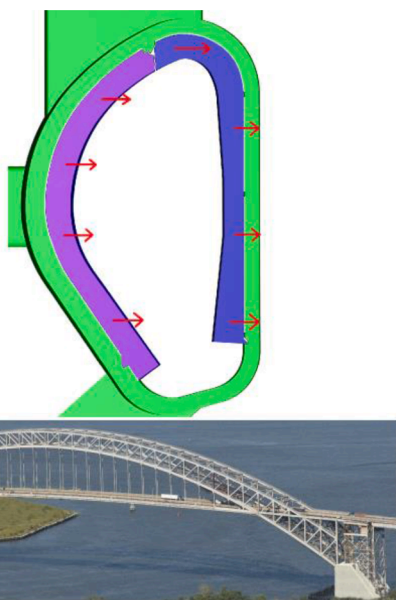


Fig. 1. Top: attachment concept of the vertical BB segments relying on the presence of radial ferromagnetic forces (red arrows). Bottom: New Jersey Bayonne bay arch bridge relying on Gravity.

forces [7]. Horizontal slits incorporated in the BB FW and breeder zone as in the previously envisaged multi-module segment design concept [14, 15] are not required.

It had initially been assumed that during operation the ferromagnetic force would ensure physical contact on the radial supports of the blanket segments in all load cases. Instead it was found that EM forces due to a plasma thermal quench, a fast plasma current quench and due to a fast discharge of the TF coils may exceed the ferromagnetic force on some BB segments, see Table 3. Consequently, the BB segments must be supported at the top and at the bottom in both radial directions. This fact also disqualifies the radial supports from being used as electrical connection to the VV since the electrical configuration would become unreliable. Instead we rely on the vertical supports as electrical connection. The radial supports will be electrically insulated, see paragraph 1.2.

#### b) Vertical pre-compression by obstructed thermal expansion

After installation of the BB segments a small gap of  $\sim 20\text{mm}$  remains at their upper vertical supports that is insufficient to allow free thermal expansion of the segments when heated up in standby state to  $\sim 300^\circ\text{C}$ . Hence prior to plasma ramp-up the BB segments are vertically clamped in-between their upper and lower vertical supports. During plasma operation the clamping force will further increase as the plasma-facing areas of the BB heat up more than the backside. Thus, physical contact between VV and BB is guaranteed and the vertical supports can be relied upon for electrical connection.

#### c) Supports in shutdown state

At machine shutdown the TF coils are discharged and the ferromagnetic force does no longer act. The BB cooling systems are either idle or operate at low flow and at much reduced temperature. The BB segments have thermally contracted and lost contact at their upper vertical supports. Consequently, the support constraints are different: the BB segments are vertically supported at the bottom and toroidally constrained by shear keys. Radial stops at the upper vertical supports prevent the BB segments to fall off the VV wall due to the location of their centers of gravity or during a seismic event.

### 1.4. Electrical connections

Each BB segment is electrically grounded to the VV at the vertical supports. Electrical connections between BB and VV being both at the top and at the bottom ensures the path of halo currents inside the BB segments to be relatively short. The gap between the BB segments is sufficiently large to prevent contact also considering mechanical or thermal deformations. The electrical configuration is therefore defined and electrical currents can flow from one BB segment to another only through the VV or the plasma.

The electrical connections between VV and BB rely on physical contact of the corresponding metallic surfaces that is provided by the vertical pre-compression due to the BB thermal expansion. The electrical contact resistance will need to be assessed by a specific R&D program. Where vertical supports exist on both lateral sides of a BB segment one of the two is electrically insulated to avoid net toroidal currents entering into the BB segment on one side and exiting on the other.

### 1.5. Machine states and fabrication tolerances

The gaps around the BB segments are rather small ( $\sim 20\text{mm}$ ). Also the clearances at the supports must be small during operation to avoid dynamic amplification of the large electromagnetic (EM) loads acting on the BB, typically not larger than  $\sim 0.5\text{-}3\text{mm}$  depending on the relevant BB natural frequency [17, 18]. Given the BB's considerable dimensions and temperature variations, see Table 1, the scale of its relative thermal expansion to the VV is similar and - in some cases - exceeds the dimensions of these clearances. A number of machine states must

**Table 1.**

Toroidal field, VV and BB temperatures in different machine states.

State	TF	T <sub>VV</sub>	T <sub>BB</sub>
IVC installation	OFF	20°C	20°C
Baking	OFF	180°C	240°C
Standby	ON	50°C	~300°C
Flat top	ON	50°C	~[300-500°C], [19]
Ex-vessel LOCA	ON	50°C	~[300-585°C] (initially), [20] ~550°C (after ~1h), [21]
BB maintenance	OFF	20°C	~[50-80°C], [22]

therefore be considered in the definition of the BB support concept to control the clearances and also to avoid excessive reaction forces due to obstructed thermal expansion.

The reasonably achievable shape tolerances of the BB and the VV are expected in the range  $\pm 5$ -20mm based on fabrication experience of the ITER VV [23]. These are larger than the required precision of the clearances at the BB supports. It is therefore foreseen to custom-machine the BB supports contact surfaces after fabrication and survey as applied on the contact pads of the outer intercoil structure of the JT60SA magnets [24]. A final precision in the mm and sub-mm range is expected, see chapter 2.1.

### 1.6. Vertical segment removal kinematics

#### a) Vacuum vessel architecture

The VV is a double-shell structure made of austenitic steel 316L(N)-IG and described in [6]. Each of its 16 sectors integrate one lower horizontal port, one upper vertical port for BB replacement, and one equatorial port hosting plasma heating and/or diagnostic systems or a ramp-up limiter.

The VV is a toroidally continuous conductive structure in proximity of the plasma. Plasma vertical excitations induce toroidal currents in the VV providing passive stability to the plasma. Since the toroidal continuity is interrupted by the VV ports the inner shell above and below the equatorial ports is particular important in this respect.

Each VV upper port provides direct access to the back-side of five BB segments and allows servicing the BB pipes and connecting the BB transporter to the BB. The size of the upper port is limited by the magnet coils [25]. As a result parts of the BB segments are outside the port contour, see Fig. 2. Hence, before vertical extraction through the upper

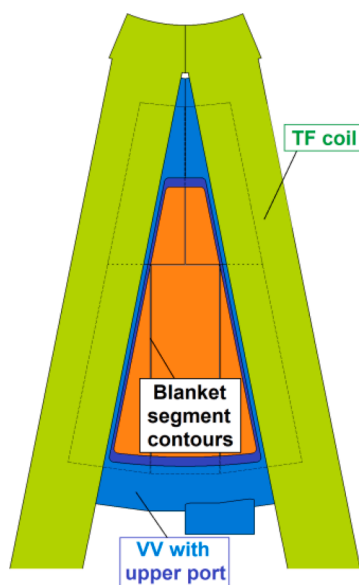


Fig. 2.. Horizontal cut through one DEMO upper port with adjacent TF coils limiting the port size and contours of the 3 outboard and 2 inboard blanket segments.

port lateral outboard segments must be translated toroidally, inboard segments must be translated both toroidally and radially. The presence of the VV inner shell above the equatorial port (as required for passive plasma stability) requires the outboard segments to be swung about the toroidal axis to fit through the upper port, see Fig. 3.

#### b) Removal sequence

Prior to the removal of any BB segment the divertor cassettes located beneath need to be removed through the lower port to free the space needed for the aforementioned translations. In addition limiters and possibly in-vessel diagnostics may obstruct the BB kinematics and hence require removal. The preparations in the upper port for the removal of the BB segments include: (i) Opening of the bioshield top lid and (ii) docking of different casks to the VV upper port for the removal of components inside the upper port (vacuum closure plate, pipe work, upper port plugs [26]).

The first segment to be removed must be the central outboard segment. Subsequently, either of the two lateral outboard segments can be removed. The removal of one of the inboard segments requires prior removal of the central and one lateral outboard segment.

#### c) Removal kinematics

**Outboard segments:** To disengage an outboard segment from its lower support it needs to be lifted by  $\sim 120$ mm and tilted about the toroidal axis by few degree. The inboard segments are still in-situ while the outboard segments are being removed. To prevent collision with the inboard segments during the vertical lift into the cask the outboard segments must be tilted back at mid-height (step 3 in Fig. 3). Since the inboard side of the upper port is narrow its toroidal width is increased above the level of poloidal field coil 1 (PF1) to provide the space required for this tilt.

**Inboard segments:** To disengage an outboard segment from its lower support it needs to be lifted by  $\sim 20$ mm and tilted about the toroidal axis by few degree. The following translations of the inboard segment must comply with the VV contour that encloses the segment on the top. Inboard segments must therefore be lowered with an angle of about  $45^\circ$  into the divertor region (step 2 in Fig. 3). This translation must be far enough to clear the poloidal contour of the residual inboard segments to allow for a toroidal translation to the center of the VV sector. A 2<sup>nd</sup> vertically inclined translation (step 4) then moves the inboard segment further towards the outboard and below the upper port allowing for the vertical lift into the cask.

## 2. Design description

### 2.1. Custom-machining of BB supports structures

**Custom machining of all VV support structures** after VV assembly in the tokamak pit is foreseen. Up to  $\sim 40$ mm of material can be removed from the contact surfaces of the VV supports allowing the correction of the VV shape deviations by  $\pm 20$ mm, see Fig. 4. First, the as-built VV inner shell is surveyed and the VV support structures are adjusted to the global machine coordinate system. The expected precision after this first step is  $\pm 1.5$ mm, mainly caused by the imprecision within the surveying process. In a second step the VV radial supports of each inboard segment are custom-machined with respect to each other. The expected relative precision amongst the radial supports of a single inboard segment is  $\pm 0.2$ -0.4mm.

**Custom machining of all BB supports** is foreseen after the fabrication of each segment to radially adjust the BB support interfaces and correct shape deviations of the BB segment. The relative precision is expected to be as low as on the VV:  $\pm 0.2$ -0.4mm. Consequently, during operation the inboard segments are moderately bent by the ferromagnetic force closing any remaining gaps ( $\leq 0.4$ -0.8mm) and ensuring physical contact on all radial supports.

Shape deviations of the BB segment, which are expected in the range

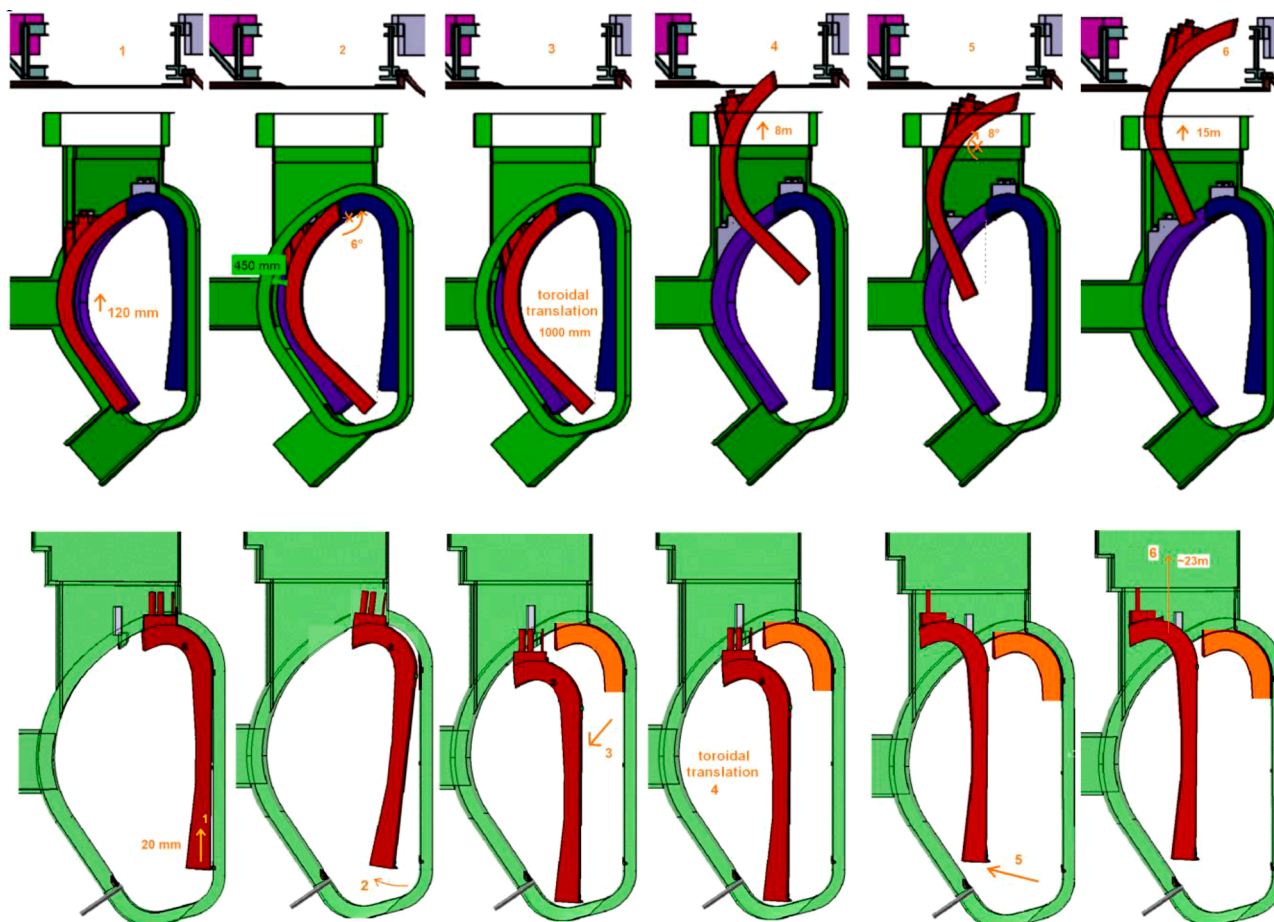


Fig. 3.. Removal kinematics of the DEMO BB vertical segments. Top: outboard segments, bottom: inboard segments.

of  $\pm 5$ -10mm, are *not* corrected, see Fig. 4. Hence the radial position of FW may deviate from the nominal and must be taken into consideration in the prediction of impact areas of charged particles on the FW.

The heat generated in the steel of the support structures by the neutron radiation will cause an elevated temperature level depending on the thickness of the steel, i.e. the distance of the surface from the coolant. The neutron flux at the location of a support structure depends on the neutron shielding provided by the IVCs. The consequent neutron heating varies approximately in the range of 0.1-0.5 W/cm<sup>3</sup> [27]. The consequent thermal stresses limit the steel thickness in the BB supports.

## 2.2. Design of the radial supports

Radial supports are implemented in all cases on both lateral sides of the BB segments, see Fig. 5 and Fig. 10. During operation the ferromagnetic force provides a pre-compression on two lateral radial supports at three and two poloidal locations on the inboard and the outboard segments, respectively. Due to the pre-compression provided by the ferromagnetic force they can support the BB segments also against vertical moments that may occur in plasma disruptions.

## 2.3. Design of the toroidal supports

In addition to radial/vertical supports each blanket segment has toroidal shear keys that engage into corresponding slots in the VV. These shear keys react the large radial moments acting on the blanket during a fast plasma current quench that occurs during a disruption. The inboard segments have two shear keys, one at the bottom and one at the top, providing a statically determined support condition.

## 2.4. Design of the vertical supports

### a) Main vertical supports

During *installation* and *in-vessel maintenance* the BB segments are at 20°C and  $\sim 50$ -80°C, respectively, see Table 1. In these states the BB segments are vertically supported on the bottom only; at the upper supports there are gaps of  $\sim 20$ mm. During plasma operation these gaps are closed and the BB segments are vertically supported also on the top.

To engage the inboard segments into their lower VV supports the final installation movement is a vertical drop of  $\sim 20$ mm, see Fig. 9. The final installation movement of the outboard segments is a vertical drop of  $\sim 120$ mm, see Fig. 3 and Fig. 6. Consequently, after installation a vertical gap is unavoidable above the lateral outboard segments and above the inboard segments of at least 120mm and 20mm, respectively. To avoid impact loads on the upper vertical support and high dynamic amplification of upward loads that can occur due to halo currents in upward vertical displacement events (VDEs), see Table 3, these gaps need to be closed during plasma operation. Indeed, these gaps must be closed prior to plasma operation in *standby* since VDEs may occur also during plasma ramp-up. The BB thermal expansion within the VV in *standby* will reduce the vertical gap by  $\sim 31$ mm and we rely on this to sufficiently close the  $\sim 20$ mm installation gap at the inboard segments. To close the  $\sim 120$ mm installation gap above the lateral outboard segments removable stops will be inserted after BB installation, see Fig. 7. These will be adjusted to retain a similar-size gap prior to BB heat-up as above the inboard segments ( $\sim 20$ mm).

The gap above the central outboard segments can be closed adjusting the upper port plugs that are installed after the BB.

As introduced in paragraph 1.3 during operation the BB segments are

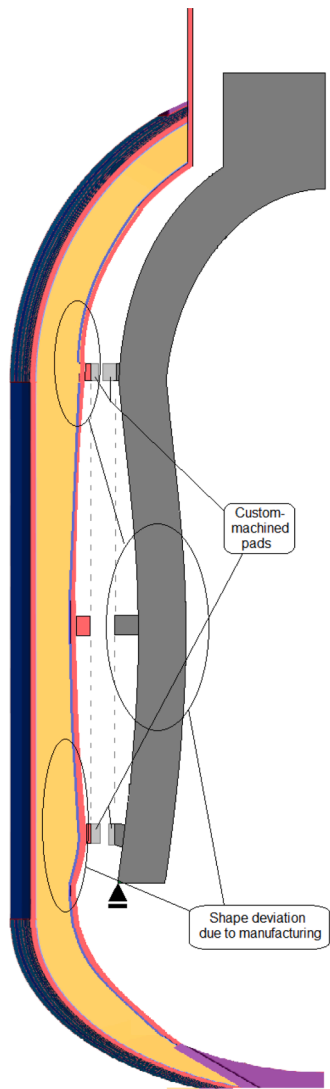


Fig. 4.. Principle sketch illustrating the foreseen custom-machining on the VV side and on the BB side to compensate manufacturing tolerances.

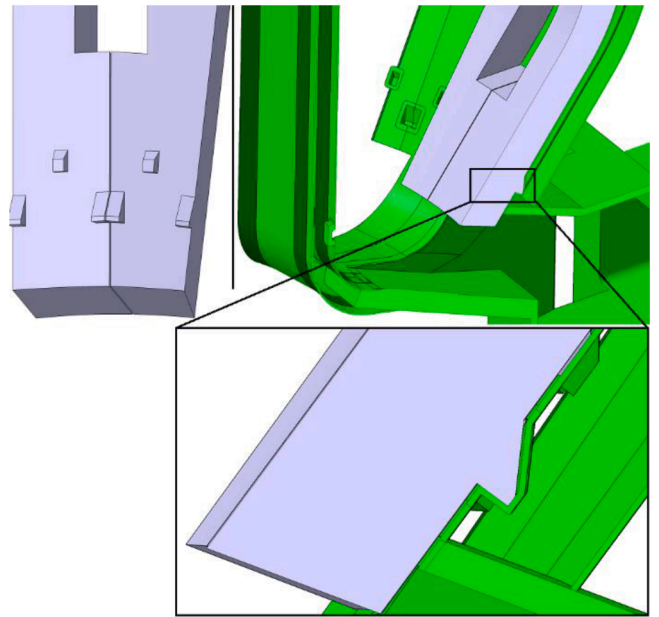


Fig. 6.. Lower supports of the outboard segments providing support in both radial directions.

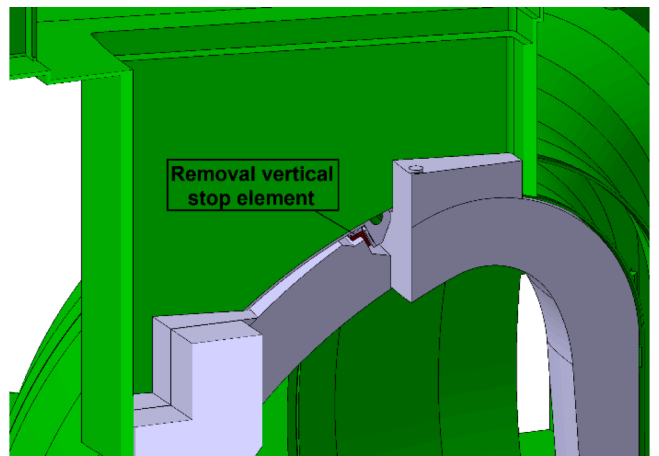


Fig. 7.. View inside the upper port with removed upper protection limiter showing the removable stop element (brown) at the upper supports of the outboard segments providing support in both radial directions, bolt for forced extraction in case of bonded contact surfaces not shown.

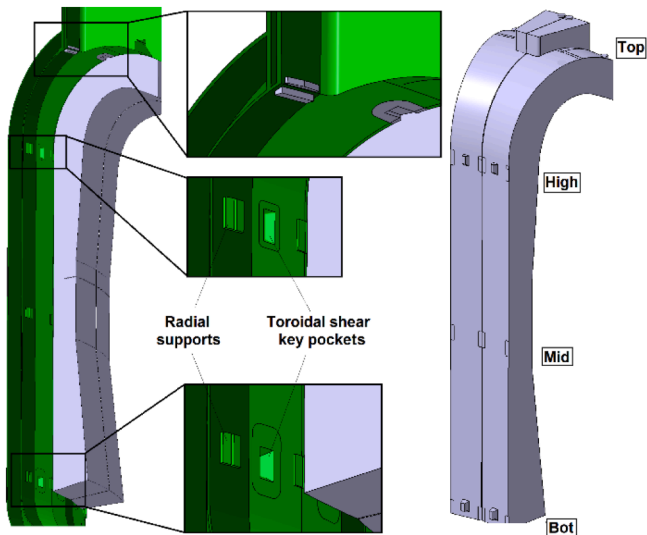


Fig. 5.. Supports of the inboard BB segments.

not free to thermally expand and their temperature state causes (secondary) stresses within the BB and reaction forces on the BB vertical supports. The potential for these reaction forces to overload the BB supports requires controlling the BB's stiffness and temperature levels in normal and upset conditions, see paragraph 3.5.

Initially it had been attempted to implement a single vertical support at the bottom of the BB reacting both upwards and downwards loads. (In radial direction the BB would have retained its supports on both, the top and the bottom.) Such a supporting concept with a constraint in a single location is conventionally chosen for components undergoing significant thermal expansion. However, since the unconstrained vertical expansion of the BB segments during normal operation is expected to be significant (~70-160mm, [28]) meeting the requirements of the BB FW alignment (paragraph 1.2) is considered impossible at the top without guaranteed contact to the VV.

b) Radial stops - inboard segments

To support the inboard segments against forces pulling them off the VV wall radial stops are integrated at the top and at the bottom supports. The radial stop at the top is provided by a surface of 30mm height on the upper support rail, see Fig. 8. In the bottom supports a vertical step of 15mm height is implemented, see Fig. 9.

2.5. Engagement and release

a) Installation

The BB transporter will position the BB segment with a tolerance of  $\sim\pm 40\text{mm}$ . During the last installation movements the BB segments are guided by the BB support structures into their installed position achieving a much smaller installation tolerance of  $\sim\pm 2\text{mm}$ . This is caused by the surveying precision of the BB supports ( $\pm 1.5\text{mm}$ ) and their custom-machining tolerances, see paragraph 2.1. The BB supports therefore have a wedged shape ensuring that during engagement into the VV pockets the gaps reduce progressively, see Fig. 10. The BB segment being installed may be attracted to a residual BB segment due to their ferromagnetism and slide across pre-defined contact areas during installation. During the engagement the BB toroidal supports enforce the separation of adjacent BB segments.

b) Release

Metal-to-metal surface bonding, called in literature also sticking, stiction or adhesion, sometimes occurs in vacuum where the reformation of destroyed oxide layers is prevented. This has often been observed in fusion machines [29] and space applications [30]. A careful choice of the type of metals at the interface and the use of dissimilar materials can reduce significantly these issues. Existing fusion machines use e.g. Al-bronze that is also foreseen in ITER [12].

To further mitigate the risk of surface bonding at the BB supports Table 2 identifies methods to break open bonded contacts at surfaces that are under constant and high compression during operation. The following procedure was identified to potentially release bonded surfaces on most BB support interfaces prior to BB removal. This procedure has not yet been validated by a suitable test program.



Fig. 9.. Horizontal cross-section in the toroidal mid-plane of the inboard segment showing the lower support.



Fig. 10.. Horizontal cross-section through the VV and the bottom support of two inboard BB segments, right: in installed position, left: prior to engagement into the shear key pocket with indication of required positioning precision, here 37mm.

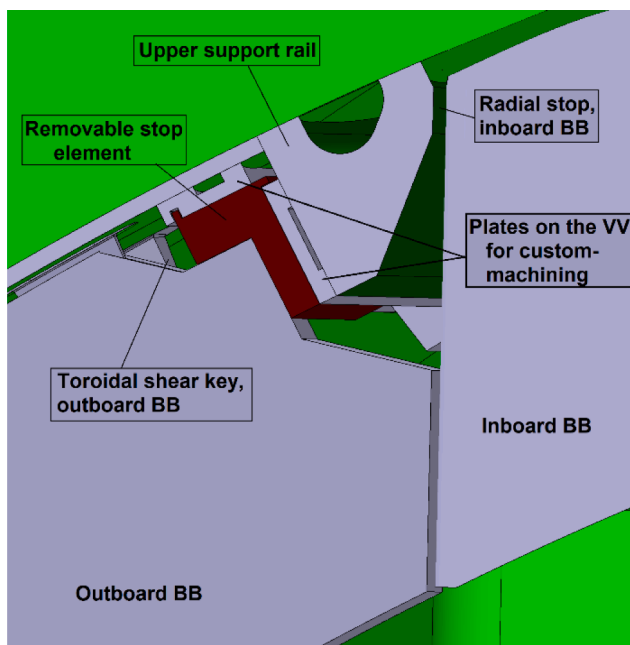


Fig. 8.. Horizontal cross-section through of the upper support rail including the radial stop of the inboard segments.

Table 2.

Methods foreseen to release metal-to-metal surface bonding prior to BB removal.

Location	Ref.	Method for release of surface bonding
Bottom vertical supports – outboard BB	Fig. 11	Toroidal BB thermal contraction
Bottom vertical supports – inboard BB	Fig. 10	none (to be defined)
Top BB vertical supports	Fig. 7	Vertical BB thermal contraction
Top BB radial supports	Fig. 11	Toroidal BB thermal contraction
Removable stop at upper supports of outboard segments	Fig. 7	Release screw
BB radial supports	Fig. 11	Toroidal BB thermal contraction

- i The magnets are discharged to terminate the ferromagnetic force acting on the BB segments.
- ii The plasma chamber is vented with dry air to prevent surface bonding to take place from this point on.
- iii The BB segments are cooled-down to  $\sim 20\text{-}100^\circ\text{C}$  using their active cooling system. In this phase the toroidal shear keys ensure the toroidal position of the BB with a precision of  $\pm 0.5\text{mm}$ . The BB supports on the lateral sides contract toroidally by  $\sim 1.5\text{mm}$  releasing bonded surfaces, see Fig. 11.
- iv The VV is opened and the BB removal sequence initiated.

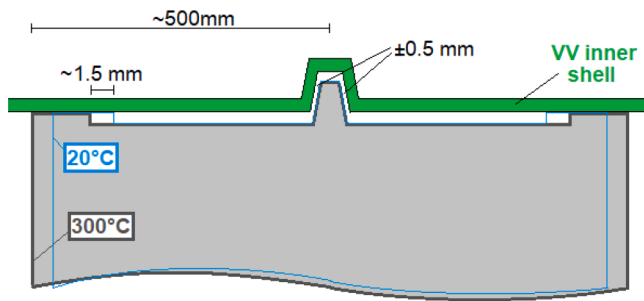


Fig. 11.. Horizontal cross-section (not to scale) through BB segment during the release procedure in case of bonded contact surfaces by on cooling down the BB from its high operational temperature (here to 20°C).

### 3. BB segment loads

#### 3.1. Accelerations

In the current reference configuration the volume of individual inboard and outboard BB segments is approximately 15m<sup>3</sup> and 21m<sup>3</sup>, respectively. The corresponding mass – assuming the heavier water-cooled lead-lithium (WCLL) concept - is approximately 125 and 180 tons, respectively. Gravity therefore generates per BB segment vertical reaction support forces of 1.25 and 1.8 MN, respectively.

During seismic events the BB segments, as they are attached to the VV, are accelerated horizontally and vertically in addition to gravity. The worst case seismic load occurs in the category IV event SL-2. It is expected to accelerate the VV in horizontal and vertical direction up to about 0.3g and 0.8g, respectively. Since plasma disruptions can accelerate the BB even more severely seismic loads are mainly relevant during machine shutdown when the toroidal field is off and the blanket support concept cannot rely on the ferromagnetic force, see paragraph 1.3.

#### 3.2. Currents induced during TF coil fast discharge

To prevent damage to the TF superconductor in case of a quench the coil current is rapidly discharged into a dump resistor. As a consequence poloidal currents are induced in the VV and the IVCs, whose electrical connections to the VV allow for net poloidal currents to flow, see Fig. 12.

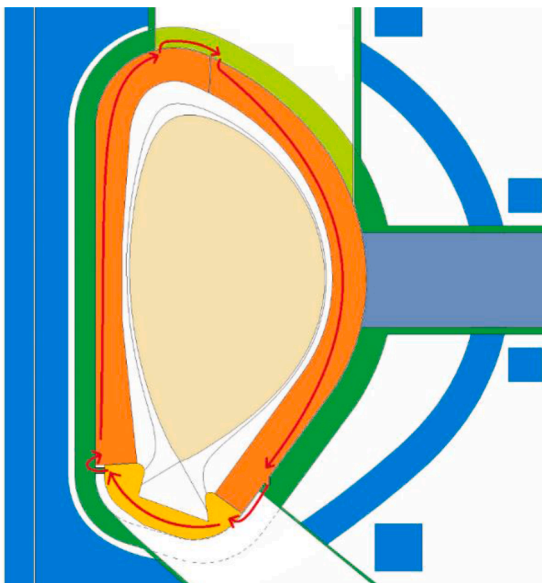


Fig. 12.. Path of induced net poloidal currents in the IVCs (red) that occur during a thermal quench and TF coil fast discharge.

Crossing the toroidal field these currents cause a pressure load directed away from the plasma that is strongest on the inboard [25].

#### 3.3. Currents induced during disruptions

##### a) Thermal quench

The thermal quench is triggered by a plasma instability causing the sudden loss of confinement. Within a very short time (in the order of ms) the toroidal flux increases and the plasma current profile flattens. Within the same time the plasma center is moved towards the inboard wall. To preserve the toroidal flux poloidal currents are induced in the components in proximity of the plasma, i.e. the FW and the divertor but also the VV.

The principle current pattern is independent from the BB support concept since the BB segments are electrically connected at the top and the bottom allowing a poloidal net current to flow through each BB segment, see Fig. 12. As in the TFCFD forces are generated on the IVCs directed away from the plasma.

##### b) Current quench

A fast plasma current quench generates a variation of the poloidal magnetic flux that induces a toroidal current in the toroidal conductive structures. These occur in primarily in the VV while they are prevented in the BB by one of the two supports on the BB lateral sides being insulated. Instead a current loop is induced causing equal-opposite poloidal forces in the sidewalls generating a very significant radial moment on each segment. This effect is well-known and has been an important design driver for the ITER IVCs [31, 32].

A previously unrecognized effect (and still under study), which can lead to large EM loads on the BB segments, is related to the toroidal asymmetry in the electrical conductivity of the VV due to the port penetrations. This was first reported in [33], which is focused on the opening in the VV due to the large upper port. Indeed, due to the consequent change in the flow pattern of the toroidal currents induced in the VV, the poloidal magnetic flux is altered in that region. Since the individual BB segments are electrically connected to the VV on the top and on the bottom, a current loop is generated in the segments of one VV

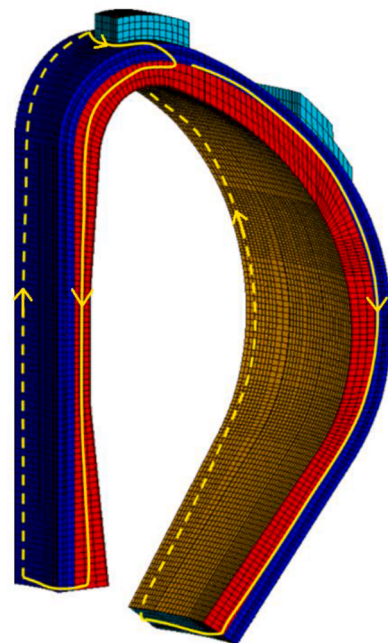


Fig. 13.. Current loops induced during the plasma current quench in the inboard and outboard BB segments of one VV sector, respectively, caused by the VV asymmetry represented by the upper port.

sector where the current flows downward in one BB segment and upwards in the other, see Fig. 13. Consequence are opposite radial forces in adjacent inboard BB segments that are large due to the length of the current path, i.e. in the range  $\pm 6$ -10MN. Such forces may overcome the ferromagnetic force and push single inboard segments away from the VV wall.

An EM analysis had been performed on a previously considered DEMO configuration with minor differences to the current configuration regarding EM loads [34, 35]. This assessment found that the current loop shown in Fig. 13 could be significantly suppressed if the toroidal continuity of the VV shells was constituted restoring the cylindrical symmetry of the poloidal flux. Toroidal electrical connectors incorporated in the upper port plug at the level of the VV inner shell to reduce the asymmetry caused by the upper port did however not significantly reduce the observed phenomenon, which will therefore remain a subject of future studies.

### 3.4. Summary of EM loads

An overview of the main EM loads acting on the BB structure is reported in [36]. They may occur due to the following phenomena: (i) interaction of the magnetic field with the BB ferromagnetic steel mainly causing forces in radial direction due to the toroidal field gradient, (ii) currents induced in the BB segments as a consequence of magnetic field variations, mainly due to a TFCFD, a plasma thermal quench or a plasma current quench (CQ), and (iii) currents from the plasma halo region running in the BB during VDEs.

Argentinian results of material irradiation indicate a decrease of the saturation of the magnetization of up to 30% due to neutron irradiation with fluences several orders of magnitude lower than what is expected in DEMO [37]. The BB support concept presented here is relatively robust against a reduction of the ferromagnetic forces since the BB is supported in both radial directions. Nonetheless, a quantification of the effect is needed to allow a complete verification of the BB support concept.

Table 3 provides an overview of the loads that drive the design of the blanket supports and is based on results from [36]. The loads along the omitted degrees of freedom occur mainly during the current quench and are of lower significance:  $F_{\text{tor}} \leq 0.3\text{MN}$  and  $M_{\text{vert}} \leq 5.0\text{MNm}$ . The EM loads are calculated based on the following assumptions:

- Each BB segment to contain about  $\sim 3.5\text{m}^3$  of Eurofer.
- TFCFD discharge time constant: 20s.
- Thermal quench time: 4 ms
- Current quench time: 74 ms, based on [38]
- Halo current: The largest halo currents in the BB are expected during a slow upward VDE. Their magnitude could in principle be extrapolated from the ITER specification, see [38]. However, the presence of protruding limiters may significantly reduce the halo currents in the BB segments. We assume here that the loads due to a TFCFD are significantly more severe hence halo current loads are not addressed specifically.
- The design of the BB is assumed as a box whose walls have equivalent electrical conductivity properties according to Fig. 14:

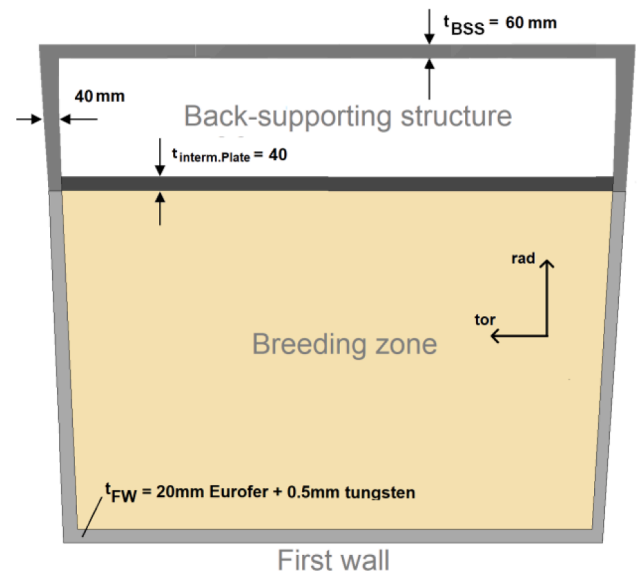


Fig. 14.. Simplified cross-section of BB segment with wall thicknesses as considered in the EM analysis.

### 3.5. Thermal conditions

**Flat top plasma operation:** During plasma ramp-up the neutron flux progressively increases and volumetrically heats the BB. In addition the heat radiated from the plasma heats the FW surface. The BB thermal capacity delays the establishment of the steady-state temperature condition in the BB. This transient phase has not been considered in this work. The steady-state BB thermal condition also depends on the outlet temperature of the BB coolant:  $\sim 328^\circ\text{C}$  in case of water and  $\sim 500^\circ\text{C}$  in case of helium. In the verification of the BB supports we considered the more extreme temperature state in the range  $\sim [300-500]$ , [19], established in the case of helium, see Fig. 15. This was found to correspond to an average temperature of the FW plate of approximately  $345^\circ\text{C}$ . The BB back-supporting structure remains close to the inlet temperature  $\sim 300^\circ\text{C}$ .

**In-vessel maintenance:** During in-vessel maintenance the plasma chamber is filled with dry air at 1 bar and the BB segments to be removed are disconnected from their cooling system. The decay of radioactive isotopes generates heat in the BB that is transferred to the dry air, which naturally circulates transferring it to the cold walls of the actively-cooled VV [22]. The temperature state established in the BB is rather uniform at a moderately elevated level, see Table 1.

**Ex-vessel LOCA:** In case of an ex-vessel loss of coolant accident (LOCA) a number of BB segments lose their active cooling. A soft plasma shutdown is triggered within 3s, causing the plasma fusion power to reduce to zero within 120s. During this time the BB continues to be heated by the plasma and a maximum temperature (in the FW) of  $585^\circ\text{C}$  is predicted in [20]. After plasma shutdown the VV is filled with dry air to enable convective heat transfer between the un-cooled BB and the VV as in the case of in-vessel maintenance. After about 1h the – more or less

Table 3.

Summary of most relevant peak net EM loads [MN, MNm] acting on the BB segments (positive radial forces act away from the machine center, positive vertical forces act upwards). Negligible loads are omitted from the table, loads that do not drive the design are grayed out. Note: Each load may occur at a different instant during the transient event. Also: The distribution of these loads across the BB segments is to some degree non-uniform.

	Inboard BB				Outboard BB			
	$F_{\text{rad}}$	$F_{\text{vert}}$	$M_{\text{rad}}$	$M_{\text{tor}}$	$F_{\text{rad}}$	$F_{\text{vert}}$	$M_{\text{rad}}$	$M_{\text{tor}}$
Ferromagnetic	[-7; -6]				-2.0			
TFCFD	-12.4				3.2			
Halo current – fast VDE up	-0.9	-9.0			-0.6	2.3		
Thermal quench	[6.5; 8.5]	[-1.9; -1.4]	8.5	[7.1; 9.0]	[-3.5; -1.8]	[0.4; 0.6]	[4.5; 5.5]	[-2.8; 0.2]
Current quench – fast disr./VDE	$\pm 6$	[-1.4; 1.9]	-13	[-11; 5]	$\pm 2.5$	[-0.35; 0.2]	[8.0; 10.0]	[0.9; 2.8]

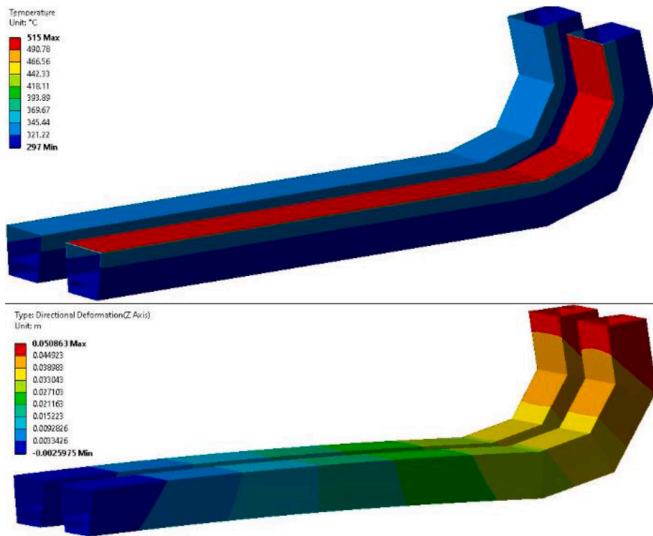


Fig. 15.. Temperature distribution during flat top and free thermal expansion of inboard BB segments. The front segment has the real 3D thermal gradient of the BB FW applied, the segment in the back the equivalent averaged FW temperature of 345°C.

uniform - temperature of the BB reaches its peak of ~500°C and ~600°C depending on the BB concept being WCLL or HCPB respectively [21].

#### 4. Verification

##### 4.1. Reaction forces

In a finite element model of a single VV sector and the corresponding two inboard and three outboard BB segments the reaction forces on the BB supports were determined for different load cases and in different machine states [7]. The reaction forces for one inboard and one lateral outboard segment are reported here and are assumed to be representative for the other segments. This holds true also for the central outboard segment in case it is not shortened to integrate and upper limiter [26]. The case of a shortened central outboard segment, which is currently thought to be supported by the upper limiter, is not covered in this article and should be subject of future design studies. Table 4 and Table 5 report the reaction forces for the machine states stand-by (with

Table 4. Reaction forces [MN] on the VV supports of an inboard segment.

Reaction force direction	Loads	Stand-by	Flat top	Ex-VV LOCA	TFCFD	Fast VDE up		Current quench	
						Thermal quench	Right BB	Left BB	Right BB
	<b>Tor. field</b>	on	on	off	on	on	on	on	on
	<b>BB temp.</b>	300°C	300-345°C	500°C	flat top	flat top	flat top	flat top	flat top
	<b>other</b>	n/a	n/a	n/a	TFCFD	VDE	VDE	VDE	VDE
Radial	Top – L	0	0	-0.3	0	0	0	0	-1.5
	Top – R	0	0	-0.2	0	-1.5	0	0	0
	High – L	1.5	1.6	0	3.6	0	0	0.5	0
	High – R	1.0	1.0	0	3.1	0	3.6	0	3.9
	Equa. – L	1.3	1.1	0	4.2	0	0	0	0
	Equa. – R	1.0	0.9	0	3.4	0	3.4	0	1.0
	Bot – L	0.8	0.9	0.3	1.8	-0.3	1.5	0.2	0
	Bot – R	0.8	0.9	0.2	2.8	-1.0	1.2	0.2	1.4
	<b>Total</b>	<b>6.5</b>	<b>6.5</b>	<b>0</b>	<b>18.9</b>	<b>-2.8</b>	<b>9.6</b>	<b>0.8</b>	<b>4.8</b>
Vertical	Top – L	-0.3	-0.4	-0.7	-0.8	0	-1.0	0	-1.3
	Top – R	-0.4	-0.6	-0.8	-0.9	-1.5	0	-0.9	0
	Bot – L	1.0	1.2	1.3	0.6	1.2	1.8	0.8	3.2
	Bot – R	1.0	1.1	1.4	0.9	2.8	0	2.2	0
	<b>Total</b>	<b>1.3</b>	<b>1.3</b>	<b>1.2</b>	<b>-0.2</b>	<b>2.5</b>	<b>0.9</b>	<b>2.0</b>	<b>1.9</b>
Toroidal	High	0.2	0.2	0	0.1	1.1	-1.4	-0.5	1.9
	Bot	-0.3	-0.3	-0.1	-0.3	-1.0	2.0	0.7	-2.5

charged TF coils), flat top, and ex-VV LOCA. The reaction forces due to the occurrence of a TFCFD or a fast upward VDE during flat top are also reported. In these tables the negative direction of the radial reaction forces acting on the VV supports is defined towards the center of the machine, positive vertical forces act downwards on the VV supports.

From the analysis results the following has been concluded:

- i **Loads during flat top and ex-VV LOCA:** The vertical loads on the top and bottom supports remain well within the design limits of the support structures. This shows that both the inboard and outboard segments are sufficiently flexible.
- ii **Loads due to TFCFD:** The TFCFD generates a high compression of the blanket segments towards the VV. On the inboard segments high support reaction forces of up to ~4 MN occur and also high stresses in the BB structure. On the outboard segments the EM load due to the TFCFD may slightly exceed the ferromagnetic force. The loads on the radial stops are however well within the design limits.
- iii **Loads during fast disruption:** Both, during thermal and fast current quench radial loads occur on some inboard and some outboard segments that exceed the ferromagnetic loads. The support condition of the inboard BB changes in this case. The inboard segment is then radially supported only on the top and on the bottom.

The determined reaction forces do not exceed the design loads of the support structures, which are as follows:

- Radial supports: ~4 MN
- Vertical supports: ~4 MN
- Toroidal supports: ~2 MN

##### 4.2. Stresses in BB segments

The stresses in the BB segments have been calculated using a finite element model. The model includes one VV sector and the corresponding 5 BB segments. These were modelled simplified using shell elements and not including internal stiffening ribs and cooling pipes. The membrane stress limit of EUROFER S<sub>m</sub> is temperature-dependent and ~160 MPa. The stress limit for primary membrane + bending stresses is ~240 MPa, that for primary and thermal stresses ~480 MPa. The stresses in the BB segments were assessed here with the aim to identify potential major issues rather than to verify the BB structural integrity. Further verifications will be required considering in greater detail the BB design incl. the detailed definition of initial gaps at supports incl. uncertainties and based on fully consistent EM analyses.

**Table 5.**  
Reaction forces [MN] on the VV supports of a lateral outboard segment.

Reaction force direction	Loads	Stand-by	Flat top	Ex-VV LOCA	TFCFD	Fast VDE up		Current quench	
						Thermal quench		Left BB	Right BB
	Tor. field	on	on	off	on	on	on	on	on
	BB temp.	300°C	300-345°C	500°C	flat top	flat top	flat top	flat top	flat top
	other	n/a	n/a	n/a	TFCFD	VDE	VDE	VDE	VDE
Radial	Top - L	0.4	0.4	0	-0.3	0.9	-0.6	1.5	0
	Top - R	0.6	0.6	-0.1	-0.7	2.1	2.5	1.4	0
	Bot - L	0.6	0.5	0	-0.1	1.3	-0.1	1.7	0
	Bot - R	0.5	0.5	0.1	-0.6	1.4	1.9	0.9	0
	<b>Total</b>	<b>2.1</b>	<b>2.1</b>	<b>0</b>	<b>-1.7</b>	<b>5.7</b>	<b>3.8</b>	<b>5.5</b>	<b>0.1</b>
Vertical	Top - L	-0.2	-0.4	-0.4	-0.1	-1.2	-2.0	-2.1	-1.3
	Top - R	-0.5	-0.7	-0.8	0	-1.2	-0.1	-0.4	0
	Bot - L	1.3	1.5	1.3	1.2	2.0	0	2.3	0.2
	Bot - R	1.4	1.6	1.6	0.6	2.7	4.2	2.2	2.5
	<b>Total</b>	<b>2.0</b>	<b>2.0</b>	<b>1.7</b>	<b>1.6</b>	<b>2.3</b>	<b>2.0</b>	<b>2.1</b>	<b>1.4</b>
Toroidal	Top	-0.1	-0.1	0	0	-0.6	-2.1	-0.5	-2.2
	Bot	0	0	0	-0.2	-0.5	-1.5	-0.5	-1

The calculated stress level in the BB segments is shown during normal operation (flat top) in Fig. 16, during an ex-vessel LOCA in Fig. 17, during a TF coil fast discharge in Fig. 18, and during a plasma disruption with fast current quench in Fig. 19.

In an ex-vessel LOCA the yield stress of ~320 MPa @ 550°C [39] is exceeded in some regions of the BB. The extend of any permanent plastic deformation needs to be well controlled as it could negatively affect the support condition and the FW alignment. During a fast current quench and during a TFCFD large stresses are generated in the inboard BB FW of up to ~300-350 MPa. Additional radial supports on the inboard wall and/or modifications of the BB design might be suitable mitigation strategies.

4.3. BB deformation/FW alignment

The positioning tolerance of the BB FW is expected to be within ±5-10mm, see chapter 2.2. The consequent increase of FW heat loads due to charged particles was found to be not higher than ~25% and hence tolerable [16]. The thermal deformation of the BB segments during operation, see Fig. 20, is mostly uniform in toroidal direction. Non-uniformities of this deformation will increase the misalignment of the FW. On the inboard side, due the higher number of supports, the FW deforms by few mm only, which is considered non-critical. On the outboard side up to 16mm are predicted at the equatorial plane. However, the presence of plasma limiters on the outboard side that protrude the BB FW [40] and its relatively large distance to the last closed flux surface of 225mm on the midplane is expected to prevent excessive heat

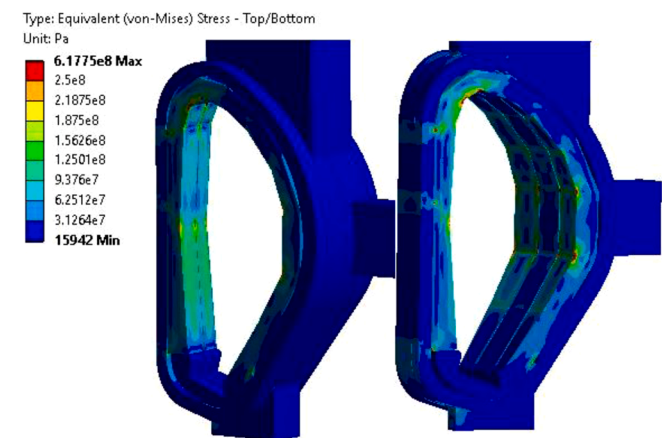


Fig. 16.. Primary + secondary membrane plus bending stress distribution in the BB segments during flat top, orange contour manually defined as 250 MPa.

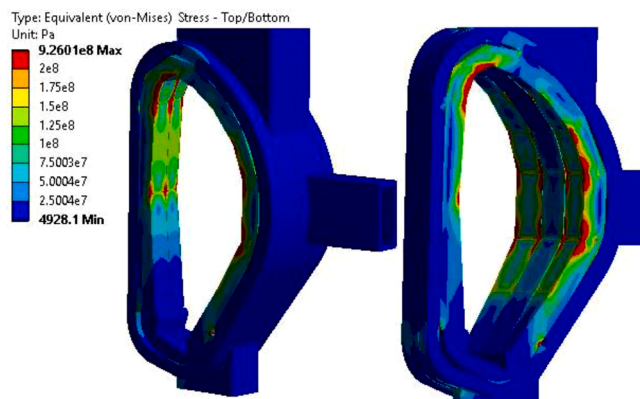


Fig. 17.. Primary + secondary membrane plus bending stress distribution in the BB segments during ex-vessel LOCA (BB temperature 500°C), orange contour manually defined as 200 MPa.

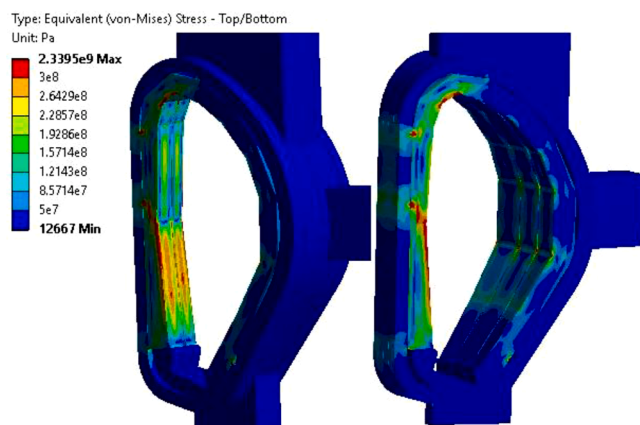


Fig. 18.. Primary + secondary membrane plus bending stress distribution in the BB segments during a TFCFD that occurs during flat top, orange contour manually defined as 300 MPa.

loads on any leading edges of the BB FW.

5. Summary

A concept of the mechanical supports for the large vertical segments of the DEMO BB has been described including the relevant machine states, loads and boundary conditions. The concept does not require

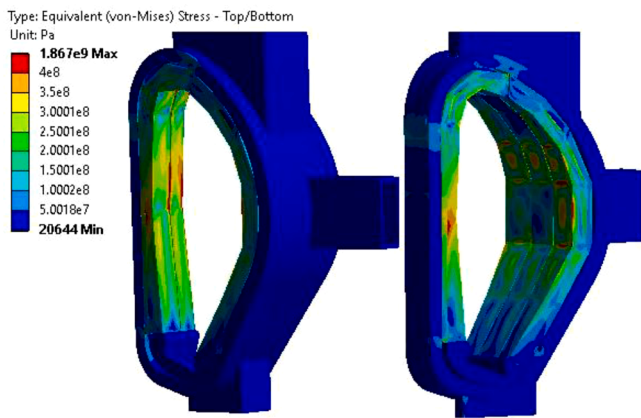


Fig. 19.. Primary + secondary membrane plus bending stress distribution in the BB segments during the fast current quench of a plasma disruption, orange contour manually defined as 400 MPa.

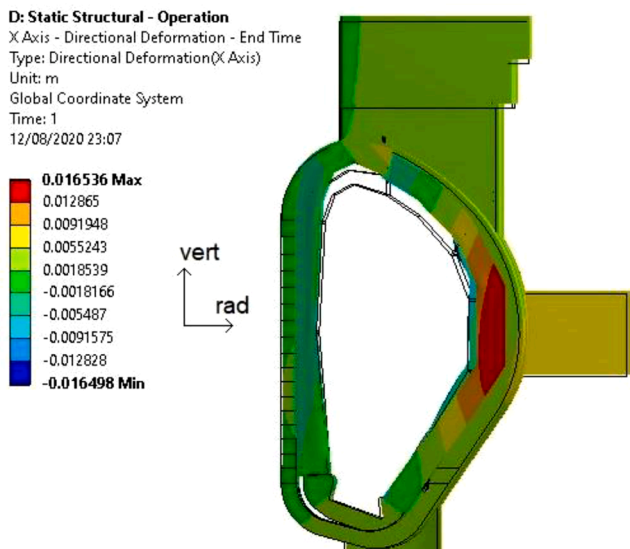


Fig. 20.. Radial displacement of the BB due to thermal deformation during flat top operation.

bolts for electrical straps of mechanical attachments requiring access and release. This greatly simplifies the remote replacement of the BB segments.

**Mechanical assessment:** The support structures on the VV and the BB segments have been assessed regarding support reaction forces, thermal and mechanical stresses in the BB and VV for the most relevant machine states and load conditions. The assessment has been carried out using models that include a number of simplifications in particular regarding the design of the BB. The verifications are therefore preliminary. The reaction forces on the support structures are within the design limitations also in case of extreme thermal expansion of the BB during an ex-vessel loss of coolant accident. Stresses in the inboard segments seem to be beyond the stress limits due to eddy current loads during a TF coil fast discharge or a fast plasma disruption. Additional radial supports on the inboard wall and/or modifications of the BB design are promising design adaptations to reduce these stresses.

**FW deformation:** The deformation of the FW during operation has been quantified and is considered sufficiently low to prevent excessive heat loads due to charged particles.

Although no show-stopper was found at this point both design and verification are not in a state that would allow concluding on the feasibility of the BB support concept presented here. Given the

attractiveness of this attachment concept in particular regarding the remote replacement complexity the following future steps are recommended for a reliable substantiation:

- Completion of the CAD design of the BB supports, in particular of those integrated in the upper port plug.
- Investigate in greater detail the required vertical gap above the inboard segment during installation considering tolerances and BB deformations. The requirement to introduce a vertical stop element as on the outboard segment can at this point not be excluded.
- Assess in greater detail the EM loads acting on the BB segments both due to its ferromagnetic material and due to induced currents. The impact of neutron irradiation on EUROFER's ferromagnetic properties needs to be quantified, too. Future EM analysis need to follow-up the design development of the BB.
- Thermal expansion of the blanket segments has not yet been comprehensively considered. Various additional thermal states of the segments need to be assessed in the future regarding asymmetric deformation and reaction forces on the supports.
- Construction of a test stand to validate the support concept on individual BB segments.

### Credit Author Statement

C. Bachmann: Conceptualization, methodology, validation, supervision, original draft

C. Gliss: Conceptualization

T. Härtl: Conceptualization

F. Hernandez: Conceptualization

I. Maione: Formal analysis, writing, review and editing, visualization

T. Steinbacher: Conceptualization, visualization

Z. Vizvary: Formal analysis, writing, review and editing, visualization

### Declaration of Competing Interest

The authors declare that they have no known competing financial interests or personal relationships that could have appeared to influence the work reported in this paper.

### Acknowledgments

This work has been carried out within the framework of the Eurofusion Consortium and has received funding from the Euratom research and training programme 2014-2018 and 2019-2020 under grant agreement No 633053. The views and opinions expressed herein do not necessarily reflect those of the European Commission.

### References

- [1] Donné, T., et al. "European Research Roadmap to the Realisation of Fusion Energy (long version)." (2018).
- [2] F. Farfaletti-Casali, et al., The interaction of systems integration, assembly, disassembly and maintenance in developing the INTOR-NET mechanical configuration, *Nuclear Engineering and Design*. Fusion 1 (2) (1984) 115–125.
- [3] Next European Torus – Introduction, executive summary, *Fusion Eng. Des.* 21 (1993) 3–15, [https://doi.org/10.1016/0920-3796\(93\)90094-X](https://doi.org/10.1016/0920-3796(93)90094-X).
- [4] ITER. IAEA, Conceptual Design Report, ITER Documentation Series 18 (1991).
- [5] D. Maisonnier, et al., Power plant conceptual studies in Europe, *Nucl. Fusion* 47 (11) (2007) 1524.
- [6] Ch Bachmann, et al., Overview over DEMO design integration challenges and their impact on component design concepts, *Fusion Eng. Des.* 136 (2018) 87–95.
- [7] Z. Vizvary, et al., Status of the DEMO blanket attachment system and remaining challenges, *Fusion Eng. Des.* 151 (2020), 111357.
- [8] F. Maviglia, et al., Effect of engineering constraints on charged particle wall heat loads in DEMO, *Fusion Eng. Des.* 124 (2017) 385–390.
- [9] D. Wilson, et al., Alignment of in-vessel components by metrology defined adaptive machining, *Fus. Eng. Des.* 98–99 (2015) 1688–1691.
- [10] M.L. Richiusa, et al., Bare and limiter DEMO single module segment concept first Wall misalignment study by 3D field line tracing, *Fusion Eng. Des.* 160 (2020), 111839.

- [11] M.L. Richiusa, et al., Poloidal distribution of penalty factors for DEMO Single Module Segment with limiters in normal operation, *Fusion Eng. Des.* 164 (2021), 112210.
- [12] A.R. Raffray, et al., The ITER blanket system design challenge, *Nucl. Fusion* 54 (3) (2014), 033004.
- [13] III.3, The NET device - Containment structures and shield, *Fusion Eng. Des.* 21 (1993) 165–212, [https://doi.org/10.1016/0920-3796\(93\)90100-V](https://doi.org/10.1016/0920-3796(93)90100-V).
- [14] A. Del Nevo, et al., WCLL breeding blanket design and integration for DEMO 2015: status and perspectives, *Fusion Eng. Des.* 124 (2017) 682–686.
- [15] Francisco A. Hernandez, et al., An enhanced, near-term HCPB design as driver blanket for the EU DEMO, *Fusion Eng. Des.* 146 (2019) 1186–1191.
- [16] Z. Vizvary, et al., DEMO First Wall misalignment study, *Fusion Eng. Des.* 146 (2019) 2577–2580.
- [17] G. Mazzone, P. Frosi, Study of dynamic amplification factor of DEMO blanket caused by a gap at the supporting key, *Fusion Eng. Des.* 98–99 (2015) 1299–1304.
- [18] S. Khomyakov, et al., Dynamic amplification of reaction forces in the blanket module attachment during plasma disruption of ITER, *Fusion Eng. Des.* 81 (1–7) (2006) 485–490.
- [19] Julien Aubert, et al., *Fus. Eng. Des.* 98–99 (2015) 1206–1210.
- [20] G. Zhou, et al., *Fus. Eng. Des.* 136 (2018) 34–41.
- [21] Draksler, Martin, et al, Analysis of the natural circulation of air inside the vented DEMO vacuum vessel after an ex-vessel loss of coolant accident, submitted to Fusion engineering and design.
- [22] Draksler, Martin, et al, "Assessment of residual heat removal from activated breeding blanket segment during remote handling in DEMO" submitted to Fusion engineering and design.
- [23] Jens Reich, et al., Three dimensional tolerance investigations on assembly of ITER vacuum vessel, in: 2009 23rd IEEE/NPSS Symposium on Fusion Engineering, IEEE, 2009.
- [24] Sam Davis, et al., JT-60SA magnet system status, *IEEE Trans. Appl. Supercond.* 28 (3) (2017) 1–7.
- [25] Ch Bachmann, et al., Issues and strategies for DEMO in-vessel component integration, *Fusion Eng. Des.* 112 (2016) 527–534.
- [26] Christian Vorpahl, et al., Initial configuration studies of the upper vertical port of the European DEMO, *Fusion Eng. Des.* 146 (2019) 2469–2473.
- [27] U. Fischer, et al., Methodological approach for DEMO neutronics in the European PPPT programme: Tools, data and analyses, *Fusion Eng. Des.* 123 (2017) 26–31.
- [28] Z. Vizvary, et al., Status of the DEMO blanket attachment system and remaining challenges, *Fusion Eng. Des.* 151 (2020), 111357.
- [29] P. Bunting, V. Thompson, V. Riccardo, Fastener investigation in JET, *Fusion Eng. Des.* 112 (2016) 42–46.
- [30] A. Merstallinger, et al., Assessment of cold welding between separable contact surfaces due to impact and fretting under vacuum, *ESA Scientific & Technical Memoranda* 279 (2009) 57.
- [31] Raffaele Albanese, et al., Electromagnetic disruption loads on ITER blanket modules, *IEEE Trans. Magn.* 46 (8) (2010) 2935–2938.
- [32] V. Amoskov, et al., Analysis of electromagnetic loads on an ITER divertor cassette, *Plasma Devices Oper.* 12 (4) (2004) 271–284.
- [33] Ivan Alessio Maione, et al., Update of electromagnetic loads on HCPB breeding blanked for DEMO 2017 configuration, *Fusion Eng. Des.* 156 (2020), 111604.
- [34] I. Maione, EM analysis of WCLL Breeding Blanket for the DEMO configuration of EUROfusion (2015) report 2018: EFDA\_D\_2NPNWM.
- [35] I. Maione, EM analysis of Breeding Blanket for the DEMO configuration of, EUROfusion (2015) report 2018: EFDA\_D\_2N4FXM.
- [36] Ivan Alessio Maione, et al., Electromagnetic analysis activities in support of the Breeding Blanket during the DEMO Pre-Conceptual Design Phase: Methodology and main results, *Fusion Eng. Des.* 166 (2021), 112285.
- [37] Rodolfo A. Kempf, et al., Correlation between radiation damage and magnetic properties in reactor vessel steels, *J. Nucl. Mater.* 445 (1–3) (2014) 57–62.
- [38] Christian Bachmann, et al., Initial definition of structural load conditions in DEMO, *Fusion Eng. Des.* 124 (2017) 633–637.
- [39] G. Aiello, et al., Assessment of design limits and criteria requirements for Eurofer structures in TBM components, *J. Nucl. Mater.* 414 (1) (2011) 53–68.
- [40] F. Maviglia, et al., Impact of Plasma Thermal Transients on the Design of the EU DEMO.", in: 14th International Symposium on Fusion Nuclear Technology (ISFNT-14), 2019.